CHIN. PHYS. LETT. Vol. 34, No. 11 (2017) 118101

Fabrication of High-Haze Flexible Transparent Conductive PMMA Films Embedded with Silver Nanowires *

Lu Zhong(钟露)[1,2], Wei Xu(许炜)[2**], Mei-Yi Yao(姚美意)[1], Wen-Feng Shen(沈文锋)[2], Feng Xu(徐峰)[2], Wei-Jie Song(宋伟杰)[2,3**]

[1]*School of Material Science and Engineering, Shanghai University, Shanghai 200444*
[2]*Ningbo Institute of Material Technology and Engineering, Chinese Academy of Sciences, Ningbo 315201*
[3]*Jiangsu Collaborative Innovation Center of Photovoltaic Science and Engineering, Changzhou 213164*

(Received 16 May 2017)

High-haze flexible transparent conductive polymethyl methacrylate (PMMA) films embedded with silver nanowires (AgNWs) are fabricated by a low-cost and simple process. The volatilization rate of the solvent in PMMA solution affects the surface microstructures and morphologies, which results in different haze factors of the composite films. The areal mass density of AgNW shows a significant influence on the optical and electrical properties of composite films. The AgNW/PMMA transparent conductive films with the sheet resistance of 5.5 Ωsq^{-1} exhibit an excellent performance with a high haze factor of 81.0% at 550 nm.

PACS: 81.07.Gf, 78.66.−w, 78.67.Uh DOI: 10.1088/0256-307X/34/11/118101

Transparent conductive films (TCF) are key components for many modern electronic devices, such as solar cells, touch panels, liquid crystal displays, and organic light emitting diodes.[1,2] Transparency and haze are two important optical parameters of TCFs, which are essential for their suitability in a particular application. The optical transmission haze is defined as the ratio of diffusive transmittance to total transmittance. Generally, optical transparency and haze factor are inversely related. The highest transmittance of the TCFs among most current reports on glass and all kinds of polymer substrates is about 90% with a very low optical haze (<10%).[3,4] Different electronic devices require different levels of light scattering. For instance, display devices need low optical haze[5] while solar-cell devices prefer high optical haze with maximized transparency.[6]

To meet the high haze requirement of the front surface of solar cells, textured TCFs are commonly used.[7,8] The morphology of the textured TCFs surfaces is usually pyramidal[9,10] or crater-like,[11,12] which were fabricated by magnetron sputtering, chemical or plasma etching, imprint lithography. Due to the particularity of the substrate in the flexible TCFs, the soft imprint lithographic method is more commonly used to prepare the high haze flexible films. However, the methods mentioned above are limited and many processes require complex steps that add cost to the solar cells devices.

Recently, silver nanowires (AgNWs) have attracted increasing interest in flexible TCFs because of their high conductivity and good flexibility properties,[13,14] as well as their excellent surface plasmon polariton.[15,16] Various flexible electronic devices have been fabricated based on AgNWs.[17,18] In this work, we focus on the preparation of the silver nanowires-based high-haze flexible TCFs. By controlling the volatilization rate of the solvent, different PMMA films with low haze and high haze are prepared. The effect of the solvent volatilization rate on film haze is studied by characterizing and analyzing the surface morphology and roughness of the PMMA films. According to this method, we prepare the AgNW/PMMA TCFs with high haze by solidifying the PMMA chloroform solution on the AgNW/glass substrates. In addition, we discuss the haze characteristics of the composite films with different sheet resistances. The low-cost and simple fabrication method for high haze flexible TCFs in this study paves the way for cost-effective production of high efficiency solar cells.

The silver nanowires (approximately 90 nm in diameter and 100 μm in length) used for this study were obtained by reducing silver nitrate in the presence of polyvinylpyrrolidone (PVP) in ethylene glycol (EG). The PVP of 0.5 g was dissolved in 50 mL EG, heated to 130℃ and stirred for 1 h. The 50 mL $AgNO_3$ solution (0.059 M in EG) was dropwise added into the flask.[19] Then a NaCl solution (50 μL 0.1 M in EG) was added and stirred for 2 min. The reaction continued for 180 min, after which it was cooled to ambient temperature. A centrifugation method (3 times at 5000 rpm) was used to remove impurities from the supernatant and separate AgNWs after adding acetone. Then several drops of AgNWs suspension were bar-coated to the glass substrates repeatedly to spread the nanowires uniformly. Subsequently, thermal treatment at 200℃ for 20 min was taken after the AgNW/glass substrates were dried at room temperature, which led to a reduction of the connection

*Supported by the International S&T Cooperation Program of China under Grant No 2015DFH60240, the Ningbo Municipal Science and Technology Innovative Research Team under Grant No 2016B10005, the Zhejiang Provincial Natural Science Foundation of China under Grant No LY15B050003, and the Ningbo Natural Science Foundation under Grant No 2016A610281.

**Corresponding author. Email: weix@nimte.ac.cn; weijiesong@nimte.ac.cn

resistance of the AgNW network.

Lastly, PMMA solution (3 wt%) with moderate viscosity was prepared by dissolving PMMA powder in chloroform, stirred for 5 min and rested for a further few minutes to remove bubbles. The pre-prepared PMMA solution was then drop-cast to the glass substrate. After being dried at 60℃ for 3 h, the films were cooled to room temperature and immersed in deionized water for 30 min, allowing it to be peeled off from the glass substrate. AgNW/PMMA composite films were prepared by dropping the PMMA solution onto AgNW-covered glass substrates.

PMMA films with two different haze factors (Figs. 1(a) and 1(b)) were prepared by controlling the volatilization rate of the chloroform solvent. After being dropped with the PMMA chloroform solution, one sample was subsequently covered with a glass petri dish (confined space can substantially lower the volatilization rate of chloroform solvent), while the other was placed in a fume hood (ventilated environment can lead to rapid volatilization of solvent). Figure 1(c) shows the transmittance and haze properties of as-prepared PMMA films. By lowering the volatilization rate of the solvent, low haze (0.6% at 550 nm, which is middle wavelength of visible light) PMMA (LH-PMMA) film with transmittance of 92.6% at 550 nm was obtained. On the contrary, high haze (76.6% at 550 nm) PMMA (HH-PMMA) film with transmittance of 89.1% at 550 nm was obtained via rapid volatilization of the solvent.

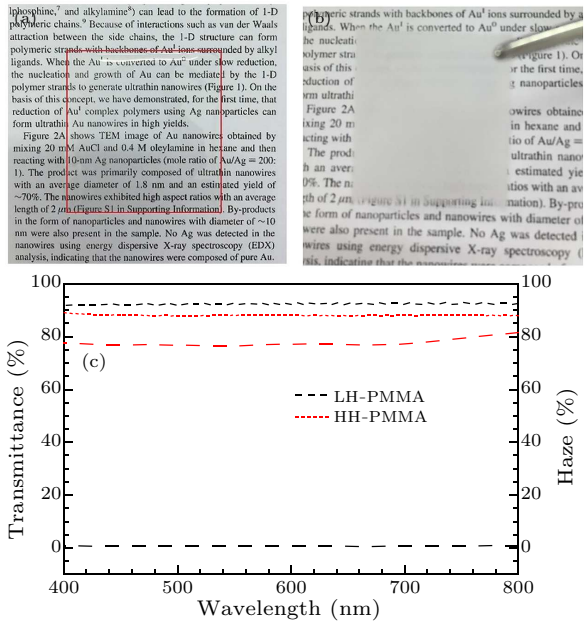

Fig. 1. The photographs of the LH-PMMA film (a) and the HH-PMMA film (b). (c) Transmittance (solid line) and haze (dotted line) properties of LH-PMMA and HH-PMMA films.

It is well known that the haze factor of thin film is affected by the surface morphology and roughness. Figures 2(a) and 2(b) show the AFM images of the upper surfaces (the side that is exposed to the air environment) of LH-PMMA and HH-PMMA films, respectively. The upper surface of the LH-PMMA film is smooth and its surface root-mean-square (RMS) roughness is only 1.62 nm (Fig. 2(c)). However, due to rapid volatilization of chloroform, a high haze phenomenon begins to appear on the PMMA film once exposed to the air environment. On the surface of HH-PMMA films, crater-like holes can be detected with an average diameter of 4 μm and an average depth of 3 μm (as shown in Figs. 2(b) and 2(d)). The RMS roughness for the HH-PMMA film increases to 917 nm, which is much higher than that of the LH-PMMA film.

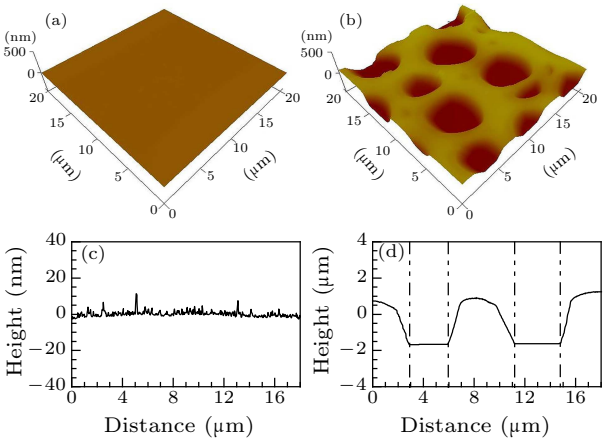

Fig. 2. AFM images of the LH-PMMA film (a) and the HH-PMMA film (b). [(c), (d)] The corresponding height distribution on one axis. The surface RMS roughness of the LH-PMMA film is 1.62 nm. The average diameter and the depth of crater-like holes on the surface of the HH-PMMA film are 4 μm and 3 μm, respectively.

A repeated spin coating process was employed to deposit the AgNWs network with different AgNW densities on the glass substrate (as shown in Figs. 3(a)–3(c)). With the software ImageJ, the areal fractional coverage, i.e., the percentage of substrate surface covered by silver nanowires, can be calculated, from which the areal mass density was deduced. Thermal annealing like those reported in other references[20,21] was also carried out to reduce the sheet resistance of the AgNWs network by welding the contact points between adjacent nanowires (as shown in Fig. 3(d)). As the areal mass density increases, the AgNWs network sheet resistance gradually decreases. When the areal mass densities are 46.6 mgm^{-2}, 89.1 mgm^{-2} and 198.3 mgm^{-2}, the corresponding sheet resistance values are 51.4 Ωsq^{-1}, 15.7 Ωsq^{-1} and 5.5 Ωsq^{-1}, respectively.

The top-view SEM image (Fig. 3(e)) shows the surface of the composite HH-AgNW/PMMA film with a sheet resistance of 5.5 Ωsq^{-1}. The AgNWs formed a uniform mesh without significant nanowire density differences across the substrate, and the pre-deposited AgNW mesh was buried in the surface of the PMMA matrix. When the solidifying process is completed, HH-AgNW/PMMA films can be peeled off from the glass substrates. In Fig. 3(e), the SEM images show

that the AgNW network is well embedded and jointed into the PMMA film.

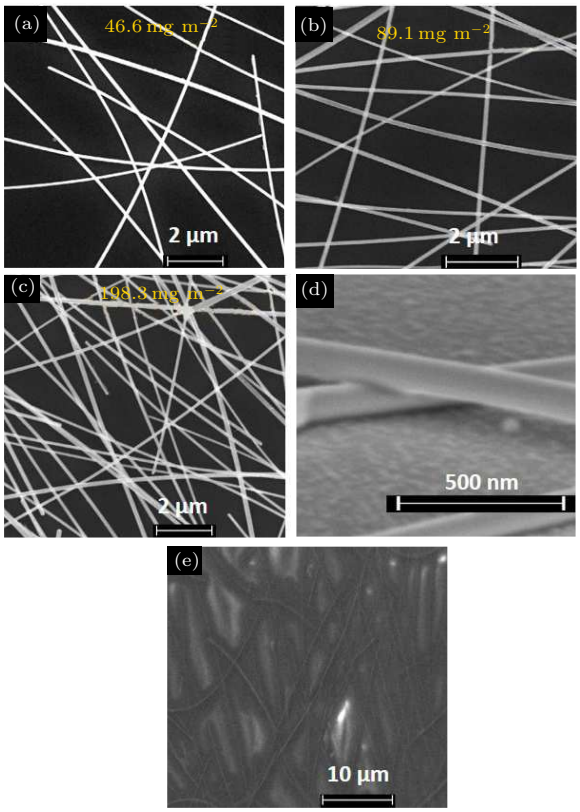

Fig. 3. (a)–(c) SEM images of AgNW network with different areal mass densities. (d) Off-angle view of the SEM image of welding phenomenon between adjacent nanowires. (e) Top-view of the SEM image of the composite film embedded with silver nanowires.

Figure 4 shows the transmittance and haze properties of HH-AgNW/PMMA films with different sheet resistances. With decreasing the sheet resistance of the composite films from 51.4 to 5.5 Ωsq^{-1}, the corresponding transmittance decreases from 87.4% to 80.2%, as the areal fractional coverage of AgNWs grows. On the contrary, the optical transmission haze of the films increases from 74.3% to 81.0% (Fig. 4(c)). As for the haze factor, it is defined as the forward scattering transmittance divided by the total transmittance, which can be calculated as follows:[22,23]

$$\text{Haze}(\%) = \frac{T_{\text{scattering}}}{T_{\text{total}}}. \quad (1)$$

Since the areal fractional coverage of AgNWs increases, light scattering caused by silver nanowires slightly strengthens, and the value of $T_{\text{scattering}}$ therefore rises accordingly. In line with Eq. (1), with increasing $T_{\text{scattering}}$ and decreasing T_{total}, the haze factor grows. For assessing the quality of those HH-AgNW/PMMA films, the figure of merit (FOM=T^{10}/R_{s}) was calculated using the sheet resistance (R_{s}) and the average transmittance T of the HH-AgNW/PMMA films.[24] The optimized HH-AgNW/PMMA film with sheet resistance of 5.5 Ωsq^{-1} and the highest haze factor of 81.0% at 550 nm shows the highest FOM value of 20.0×10^{-3} Ω^{-1} in this work.

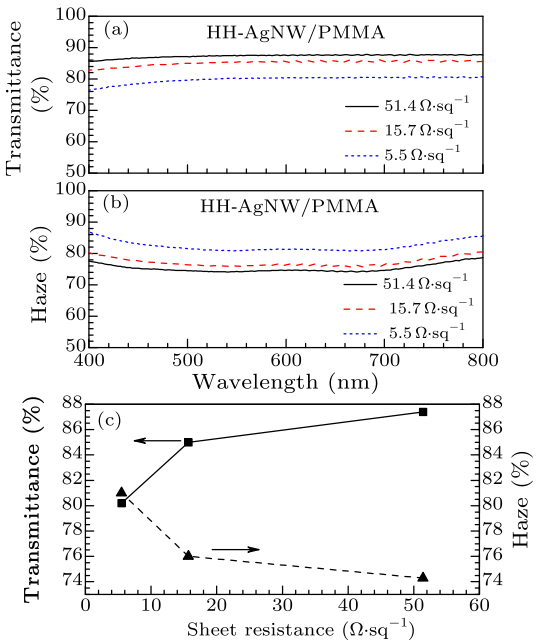

Fig. 4. Transmittance (a) and haze (b) of HH-AgNW/PMMA films with different sheet resistances. (c) The resistance-dependent transmittance and haze properties of films.

In summary, a typical high-haze flexible transparent conductive PMMA film embedded with silver nanowires has been fabricated. It is shown that the volatilization rate of a solvent during film formation can affect the surface morphology and roughness, which results in different haze factors of the films. According to the easy and low-cost process, we have prepared the AgNW/PMMA transparent conductive films (sheet resistance of 5.5 Ωsq^{-1}) with a high haze factor of 81.0% at 550 nm. This method has great potential in the cost-effective fabrication of high efficiency solar cells.

References

[1] Lee H, Lee K, Park J T, Kim W C and Lee H 2014 *Adv. Funct. Mater.* **24** 3276
[2] Wang H H 2012 *Physics* **41** 783 (in Chinese)
[3] Cui F, Yu Y, Dou L T, Sun J W, Yang Q, Schildknecht C, Schierle-Arndt K and Yang P D 2015 *Nano Lett.* **15** 7610
[4] Lee S J, Kim Y H, Kim J K, Baik H, Park J H, Lee J, Nam J, Park J H, Lee T W, Yi G R and Cho J H 2014 *Nanoscale* **6** 11828
[5] Liu Z, Xu J, Chen D and Shen G Z 2015 *Chem. Soc. Rev.* **44** 161
[6] Liu J M, Chen X L, Fang J, Zhao Y and Zhang X D 2015 *Sol. Energ. Mater. Sollar Cells* **138** 41
[7] Chen J D, Cui C H, Li Y Q, Zhou L, Ou Q D, Li C, Li Y F and Tang J X 2015 *Adv. Mater.* **27** 1035
[8] Wang K X, Yu Z F, Liu V, Cui Y and Fan S H 2012 *Nano Lett.* **12** 1616
[9] Krc J, Lipovsek B, Bokalic M, Campa A, Oyama T, Kambe M, Matsui T, Sai H, Kondo M and Topic M 2010 *Thin Solid Films* **518** 3054

[10] Wooh S, Yoon H, Jung J H, Lee Y G, Koh J H, Lee B, Kang Y S and Char K 2013 *Adv. Mater.* **25** 3111
[11] Chen X L, Li L N, Wang F, Ni J, Geng X H, Zhang X D and Zhao Y 2012 *Thin Solid Films* **520** 5392
[12] Kim D S, Park J H, Shin B K, Moon K J, Son M, Ham M H, Lee W and Myoung J M 2012 *Appl. Surf. Sci.* **259** 596
[13] Kou P F, Yang L, Chang C and He S L 2017 *Sci. Rep.* **7** 42052
[14] Shen Y and Yao R H 2016 *Chin. Phys. Lett.* **33** 037801
[15] Fang Z Y, Fan L R, Lin C F, Zhang D, Meixner A J and Zhu X 2011 *Nano Lett.* **11** 1676
[16] Fang Z Y, Lu Y W, Fan L R and Zhu X 2010 *Plasmonics* **5** 207
[17] Woo J S, Sin D H, Kim H, Jang J I, Kim H Y, Lee G W, Cho K, Park S Y and Han J T 2016 *Nanoscale* **8** 6693
[18] Yao S S, Myers A, Malhotra A, Lin F, Bozkurt A, Muth J F and Zhu Y 2017 *Adv. Health. Mater.* **6** 1601159
[19] Huang Q J, Shen W F, Fang X Z, Chen G F, Yang Y, Huang J H, Tan R Q and Song W J 2015 *ACS Appl. Mater. Interfaces* **7** 4299
[20] Lagrange M, Langley D P, Giusti G, Jiménez C, Bréchet Y and Bellet D 2015 *Nanoscale* **7** 17410
[21] Kang S, Kim T, Cho S, Lee Y, Choe A, Walker B, Ko S J, Kim J Y and Ko H 2015 *Nano Lett.* **15** 7933
[22] Han J, Yuan S, Liu L, Qiu X F, Gong H B, Yang X P, Li C C, Hao Y F and Cao B Q 2015 *J. Mater. Chem.* A **3** 5375
[23] Preston C, Xu Y L, Han X G, Munday J N and Hu L B 2013 *Nano Res.* **6** 461
[24] Van Deelen J, Klerk L A, Barink M, Rendering H, Voorthuijzen P and Hovestad A 2014 *Thin Solid Films* **555** 159